




Anisometric Iron Oxide-Based Nanoparticles and Sols Based on Them: Preparation and Properties

S. V. Stolyar^{1,2} · O. A. Bayukov³ · L. A. Chekanova³ · Y. V. Gerasimova^{1,3} · A. E. Sokolov^{1,3} · R. S. Iskhakov³ · R. N. Yaroslavtsev^{1,3}  · M. N. Volochaev³ · A. S. Artemyeva¹ · E. V. Cheremiskina¹ · Y. V. Knyazev³

Received: 14 June 2018 / Accepted: 20 June 2018 / Published online: 29 June 2018
© Springer Science+Business Media, LLC, part of Springer Nature 2018

Abstract

We have synthesized magnetic powders of the magnetite-maghemite series by the chemical reaction of the FeSO_4 iron salt and the natural arabinogalactan polysaccharide. These particles with a high magnetization value (~ 300 Gs) represent a mixture of spherical particles and nanorods. Particles of a spherical shape (diameter of ~ 5 – 6 nm) show a superparamagnetic behavior at room temperature, while rods with a diameter of ~ 5 nm and a length of 30 nm are magnetic. We have prepared sol samples based on the nanoparticle aqueous solution of arabinogalactan. Our results on the magnetism of the circular dichroism (MCD) on sol are consistent with the of Mössbauer spectroscopy data.

Keywords Nanoparticles and nanorods · Chemical preparation · Superparamagnetism

1 Introduction

Magnetic nanoparticles have a highly active surface, which leads to a high sorption ability of such samples. Due to that, they could be used as (1) carrier materials for targeted drug delivery and (2) highly specific and highly sensitive biosensors and sorbents to detect or search biomolecules in a biological fluid [1–5]. The caloric effects of the magnetized nanoparticles conditioned by the magnetic field energy dissipation were found during the magnetic relaxation processes at frequencies of ~ 1 MHz [6]. However, for low nonthermal frequencies (~ 1 kHz), the mechanical oscillations of the magnetic nanoparticles occur.

The oscillating nanoparticles in the magnetic field have the collinear magnetic moments. In the case of attaching to the biological cell membrane, these particles could be used in a nanoscale surgery as a knife for cell destruction in an alternating magnetic field [7–11]. The same effect

could be obtained by an individual anisometric particle of a rod shape. The first challenge of this study is to invent a technology of the anisometric iron oxide nanoparticle synthesis. And the second challenge is to study the structural features and magnetic properties of these nanoparticles and their sols.

2 Samples and Experimental Techniques

Magnetic nanoparticles were produced by chemical precipitation. The chemical reaction was carried out on the FeSO_4 and the natural water-soluble arabinogalactan polysaccharide (Ametis JSC, Russia) [12]. Arabinogalactan also served as a stabilizing matrix in the preparation of the sol. The preparation of iron oxide nanoparticles was based on the solution of the following composition: iron sulfate at 50 g/l, arabinogalactan at 40 g/l, NaOH at 80 °C, and pH 10. The temperature was controlled by a water thermostat. Then, we washed the resulting precipitate to a neutral pH value and dried to obtain powder. Supersonic treatment of the arabinogalactan water solution was used to sol preparation.

To study structural and magnetic properties, numerous techniques were used. Structural studies were performed by X-ray phase analysis ($\lambda = 1.54$ Å) and transmission electron microscopy (Hitachi S5500). The magnetic properties were studied by the ferromagnetic resonance method at

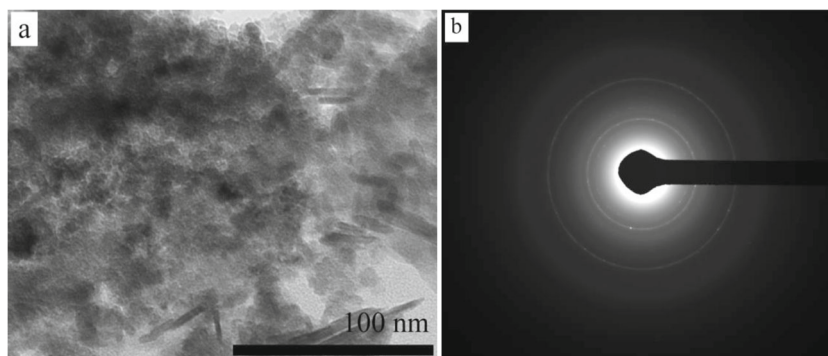
✉ R. N. Yaroslavtsev
yar-man@bk.ru

¹ Siberian Federal University, Krasnoyarsk, Russia

² Krasnoyarsk Scientific Center, Federal Research Center KSC SB RAS, Krasnoyarsk, Russia

³ Kirensky Institute of Physics, Federal Research Center KSC SB RAS, Krasnoyarsk, Russia

Fig. 1 The TEM image shows the nanorod evidence in the synthesized samples (a) and microdiffraction of the obtained samples (b)



a frequency of $f = 9$ GHz and Mössbauer spectroscopy (conventional spectrometer MS1104Em with $^{57}\text{Co}(\text{Rh})$ source). Velocity calibration of the spectrometer was carried out with an iron oxide absorber at room temperature. The nanoparticles' sol with arabinogalactan-stabilizing matrix was investigated by magnetic circular dichroism (MCD) and IR spectroscopy (Vertex 70, Bruker) with the frequency range of $700\text{--}3500\text{ cm}^{-1}$.

3 Results and Discussion

3.1 Diffraction and TEM

Figure 1 shows the results of transmission electron microscopy. It can be seen from Fig. 1a that the obtained nanoscale sample is a mixture of two types of particles: the first type is spherical particles with an average diameter of $\sim 5\text{--}6$ nm and the second is rods with a diameter of ~ 5 nm and a length of ~ 50 nm. The electron microdiffraction patterns (Fig. 1b) demonstrate two reflections with $d_1 = 2.52\text{ \AA}$ and $d_2 = 1.48\text{ \AA}$, which are consistent with two low-intensity reflections of interplanar distances d_1 and d_2 , obtained by powder X-ray diffraction patterns. According to the Scherrer formula in spherical particle assumption, the coherent scattering region is 13 nm. Unfortunately, this method does not allow us to determine the powder phase unambiguously because of the similar reflections of iron oxide polymorphs ($\alpha\text{-Fe}_2\text{O}_3$, $\gamma\text{-Fe}_2\text{O}_3$, or Fe_3O_4).

3.2 Ferromagnetic Resonance

Figure 2 shows a differential ferromagnetic resonance curve recorded at room temperature. The resonance field $H_R \approx 2900$ Oe could be denoted by the equation of $H_R = 2\pi f/\gamma$, where $\gamma = 1.7 \cdot 10^7$ Hz/Oe, line width of $\Delta H = 1600$ Oe. To determine the magnetization (M), we used a standard sample of the magnetite Fe_3O_4 ($M = 450$ G). The area under the microwave absorption curve is proportional to the sample weight and its

magnetization value. According to our calculations, the magnetization value is ~ 300 G. This value do neither coincides to the magnetite saturation magnetization value nor the magnetization of maghemite ($\gamma\text{-Fe}_2\text{O}_3$), which is 240 G at room temperature in the field $H = 10$ kOe [13]. Such behavior could be observed if particle sizes are less than 50 nm. Due to the huge surface influence, an apparent phase composition identification is hard to realize [14]. It was shown [14] that the particles of the size greater than 60 nm have a crystal structure and exhibit the physical properties of a massive magnetite with a lattice parameter $a = 0.8383$ nm. The iron oxide nanoparticles of a lesser diameter are a nonstoichiometric compound of the magnetite-maghemite mixture with the crystal chemical formula $\text{Fe}^{3+}[\text{Fe}_{1-3n}^{2+}\text{Fe}_{1+2n}^{3+}\phi_n]\text{O}_4$, where ϕ is a vacancy and n is the formula coefficient [14]. If the particle size is less than 10 nm, maghemite phase is preferable (the share

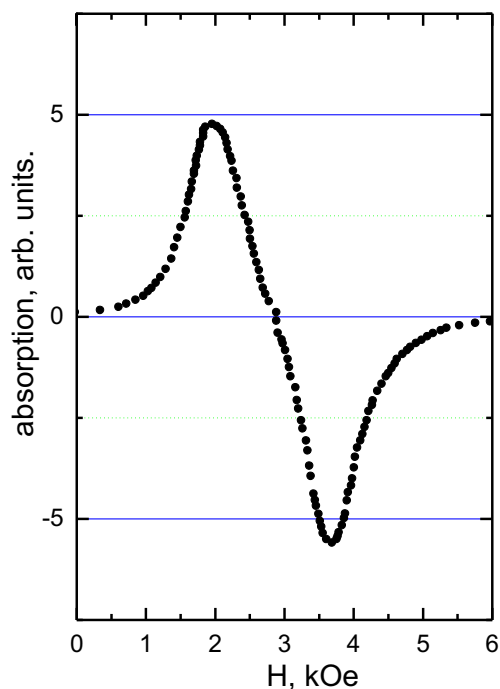
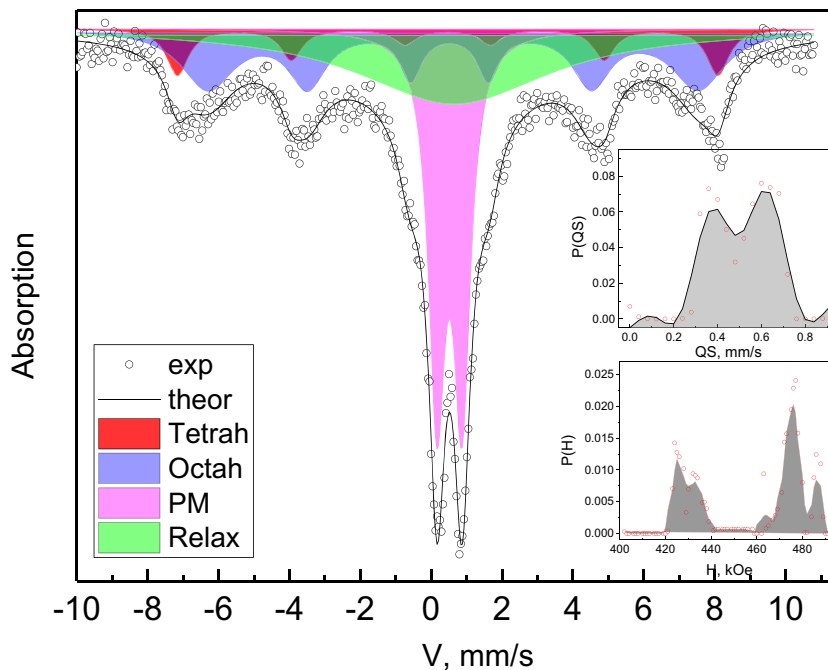


Fig. 2 The FMR spectrum of the prepared nanoparticles

Fig. 3 Mössbauer spectrum of anisometric nanoparticles. Components of the spectrum are shown by filled areas. Insets show the distributions of quadrupole splitting (QS) and hyperfine field (H)



of vacancies is 10.7%, the lattice parameter $a = 0.8361$ nm (2).

3.3 Mössbauer Spectroscopy

The Mössbauer spectrum of the studied nanoparticles at room temperature is shown in Fig. 3. The distributions of the quadrupole splitting (QS) and hyperfine field (H) are shown in Fig. 3 (see inset). According to the graphs, there are at least two distinct magnetic states of iron cations which correspond to separate probability peaks at 430 and 470 kOe. The quadrupole splitting probability calculation also predicts two distinct crystallographic states, which correspond to the superparamagnetic iron state. The modeling of the Mössbauer spectrum shows that the samples have a wide variety of the particle range.

The spectrum parameters are shown in Table 1. The spectrum component, which characterizes the superparamagnetic part of magnetic nanoparticles with blocking tempera-

tures close to room temperature, is approximated by a wide singlet ($IS = 0.49$ mm/s and relative area $A = 0.33$) and indicated in the table as “relax”. A third of the iron atoms in the nanoparticles have a blocking temperature below room temperature. This part of the spectrum was fitted by a paramagnetic doublet with the parameters $IS = 0.36$ mm/s, $QS = 0.71$ mm/s, and the relative area $A = 0.28$. Almost a third of the iron atoms are in nanoparticles with blocking temperatures above room temperature. These states are characterized by two sextets of magnetic iron atoms in tetrahedral and octahedral positions. The parameters of the Mössbauer spectrum coincide with the corresponding parameters of the maghemite powder $\gamma\text{-Fe}_2\text{O}_3$ [15, 16]. According to the paper [16], the spherical particles with the average diameter of 5.7 nm at room temperature show a superparamagnetic behavior. Our powders consist of two kinds of particles: the spheres with the diameter of 5–6 nm and the rods with the length of 30 nm. Therefore, the parameters of the sextets are related to the states of the iron atoms

Table 1 Mössbauer parameters of anisometric nanoparticles

IS	H	QS	W	A	Corresponding position
0.32	474	0	0.75–0.75	0.09	Fe ³⁺ (4)
0.42	430	0.20	0.75–1.81	0.29	Fe ³⁺ (6)
0.36	–	0.71	0.57	0.28	Fe ³⁺ (PM)
0.49	–	–	6.57	0.33	Fe ³⁺ (relax)

IS is the isomer shift relative to $\alpha\text{-Fe}$ (± 0.01 mm/s); H_{hf} is the magnetic hyperfine field at Fe nuclei (± 5 kOe); QS is the quadrupole splitting (± 0.01 mm/s); W is the line-width (± 0.01 mm/s); A is the iron occupation factor ($\pm 1.5\%$)

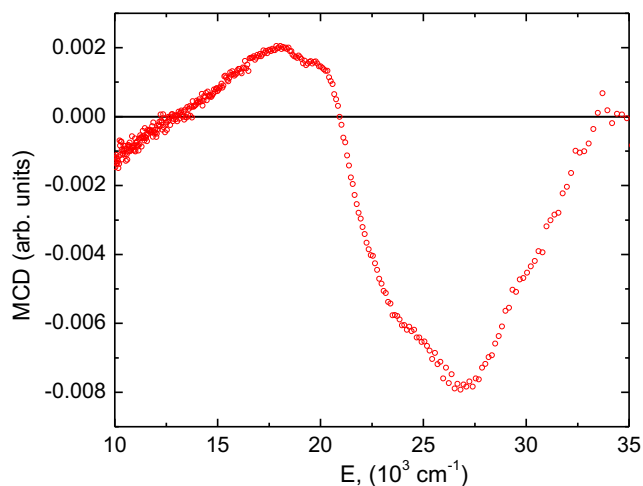


Fig. 4 MCD spectrum of the sol at $T = 300$ K

in the rods. Due to the high sensitivity of the Mössbauer spectrum, relative areas of the spherical and the rod-shape particles were obtained (Table 1).

3.4 Magnetic Circular Dichroism

The results of MCD experiments confirm our assumption of the nonstoichiometric magnetite-maghemite compounds. Figure 4 shows the MCD spectrum of the aquarabinogalactan solution of the samples in the magnetic field $H = 13$ kOe. It should be noted that the experimental curve in Fig. 4 could not be explained by either magnetite particles or maghemite particles. There are distinct specific features at $E_1 \approx 18,000$ and $E_2 \approx 20,000$ cm^{-1} . These features correspond to transitions of the Fe^{3+} ion in the tetrahedral and octahedral positions of the maghemite $\gamma\text{-Fe}_2\text{O}_3$ [17]. The wide negative maximum of the short-wavelength part agrees with the features of the magnetite MCD spectrum [17].

3.5 Infrared Spectroscopy

Infrared (IR) spectroscopy was used to study the organic matrix of the obtained sols. IR spectra of the obtained samples containing arabinogalactan were recorded at room temperature using Vertex 70 (Bruker) in the range of 370–7500 cm^{-1} . IR spectra are presented in Fig. 5. The curve *a* depicts the spectrum of the magnetic nanoparticles' sol based on arabinogalactan.

The most intensive lines correspond to the carboxyl and the hydroxyl groups with the frequencies of $\nu = 1635$ and 3304 cm^{-1} , respectively. Lines with the small intensities in the region of 1000–1200 cm^{-1} refer to the stretching vibrations of the C–O bonds and to deformation vibrations of cyclic groups. In contrast with the sol spectrum, the IR

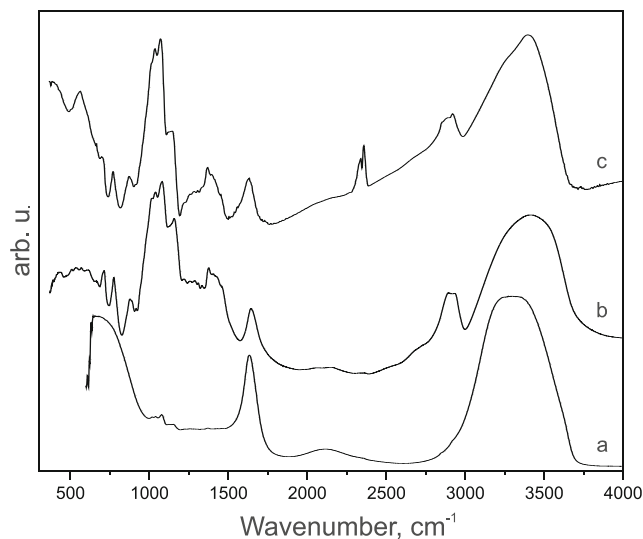


Fig. 5 IR spectra at room temperature: **a** spectrum of the magnetic sol based on arabinogalactan polysaccharide, **b** spectrum of dried arabinogalactan powder, and **c** IR spectrum of the dried sol of magnetic nanoparticles

spectrum of the dry arabinogalactan powder (Fig. 5, curve *b*) shows a decrease in the intensity of the absorption band of stretching vibrations of OH groups and the shift of its maximum to 3423 cm^{-1} as the consequence of a decrease in the number of hydrogen bonds. The spectrum exhibits the band at 2920 cm^{-1} assigned to valence vibrations of the C–H bond. There is also a decrease in the –COOH line intensity ($\nu = 1646$ cm^{-1}).

The bands of deformation vibrations with the frequencies of 700–900 and 1370 cm^{-1} are characteristic of diol alcohol groups and pyranous bonds that could be denoted as arabinogalactan IR fingerprints [18]. These vibrations are clearly observed in the IR spectrum of the sample (Fig. 5, curve *b*). The curve *c* shows the IR spectrum of the dried sol of magnetic nanoparticles. This spectrum contains the same specific features as those of dry arabinogalactan. The peak belonging to the iron oxides is observed in the region of 560 cm^{-1} .

4 Conclusion

In the present paper, we used the chemical precipitation method to synthesize the magnetic powders of iron oxides with the saturation magnetization of ~ 300 G. More than a third of the powder mass is represented by rod-shape particles with the diameter of ~ 5 nm and the length of 30 nm. The Mössbauer spectra of these rods at room temperature are characterized by two sextets corresponding to Fe^{3+} cations in tetrahedral and octahedral positions of the magnetite. However, the sample magnetization value

is lower than that of the magnetite. The MCD studies of the prepared samples confirm the Mössbauer spectroscopy results. However, there are certain issues that have not been cleared up yet and should be further studied. Due to the fact that in ultrafine particles, the surface and finite-size effects are mixed together; therefore, it is very difficult to separate them experimentally and appropriately quantify their influences.

Funding Information The reported study was carried out with the financial support of the Russian Foundation for Fundamental Research, the Government of the Krasnoyarsk Territory, and the Krasnoyarsk Territory Fund for Support of Scientific and Technical Activity in the framework of scientific Projects No. 18-43-243003, No. 17-42-240080 and No. 17-43-240527. The work is supported by the Special Program of the Ministry of Education and Science of the Russian Federation for the Siberian Federal University.

References

- Doane, T.L., Burda, C.: The unique role of nanoparticles in nanomedicine: imaging, drug delivery and therapy. *Chem. Soc. Rev.* **41**, 2885 (2012)
- Bao, G., Mitragotri, S., Tong, S.: Multifunctional nanoparticles for drug delivery and molecular imaging. *Annu. Rev. Biomed. Eng.* **15**, 253–282 (2013)
- Urries, I., Muñoz, C., Gomez, L., Marquina, C., Sebastian, V., Arruebo, M., Santamaria, J.: Magneto-plasmonic nanoparticles as theranostic platforms for magnetic resonance imaging, drug delivery and NIR hyperthermia applications. *Nanoscale* **6**, 9230 (2014)
- Reddy, L.H., Arias, J.L., Nicolas, J., Couvreur, P.: Magnetic nanoparticles: design and characterization, toxicity and biocompatibility, pharmaceutical and biomedical applications. *Chem. Rev.* **112**, 5818–5878 (2012)
- Tartaj, P., Morales, M., del, P., Veintemillas-Verdaguer, S., González-Carretero, T., Serna, C.J.: The preparation of magnetic nanoparticles for applications in biomedicine. *J. Phys. D: Appl. Phys.* **36**, R182–R197 (2003)
- Di Corato, R., Espinosa, A., Lartigue, L., Tharaud, M., Chat, S., Pellegrino, T., Ménager, C., Gazeau, F., Wilhelm, C.: Magnetic hyperthermia efficiency in the cellular environment for different nanoparticle designs. *Biomaterials* **35**, 6400–6411 (2014)
- Domenech, M., Marrero-Berrios, I., Torres-Lugo, M., Rinaldi, C.: Lysosomal membrane permeabilization by targeted magnetic nanoparticles in alternating magnetic fields. *ACS Nano*. **7**, 5091–5101 (2013)
- Connord, V., Clerc, P., Hallali, N., El Hajj Diab, D., Fourmy, D., Gigoux, V., Carrey, J.: Real-time analysis of magnetic hyperthermia experiments on living cells under a confocal microscope. *Small* **11**, 2437–2445 (2015)
- Zhang, E., Kircher, M.F., Koch, M., Eliasson, L., Goldberg, S.N., Renström, E.: Dynamic magnetic fields remote-control apoptosis via nanoparticle rotation. *ACS Nano*. **8**, 3192–3201 (2014)
- Golovin, Y.I., Gribanovskii, S.L., Golovin, D.Y., Klyachko, N.L., Kabanov, A.V.: Single-domain magnetic nanoparticles in an alternating magnetic field as mediators of local deformation of the surrounding macromolecules. *Phys. Solid State*. **56**, 1342–1351 (2014)
- Master, A.M., Williams, P.N., Pothayee, N., Pothayee, N., Zhang, R., Vishwasrao, H.M., Golovin, Y.I., Riffle, J.S., Sokolsky, M., Kabanov, A.V.: Remote actuation of magnetic nanoparticles for cancer cell selective treatment through cytoskeletal disruption. *Sci. Rep.* **6**, 33560 (2016)
- Trofimov, B.A., Sukhov, B.G., Aleksandrova, G.P., Medvedeva, S.A., Grishchenko, L.A., Mal'kina, A.G., Feoktistova, L.P., Sapozhnikov, A.N., Dubrovina, V.I., Martynovich, E.F., Tirskaa, V.V., Semenov, A.L.: Nanocomposites with magnetic, optical, catalytic, and biologically active properties based on arabinogalactan. *Dokl. Chem.* **393**, 287–288 (2003)
- Guivar, J.A.R., Martinez, A.I., Anaya, A.O., Valladares, L.D.L.S., Felix, L.L., Dominguez, A.B.: Structural and magnetic properties of monophasic maghemite (γ -Fe₂O₃) nanocrystalline powder. *Adv. Nano.* **03**, 114–121 (2014)
- Salikhov, S.V., Savchenko, A.G., Grebennikov, I.S., Yurtov, E.V.: Phase composition and structure of iron oxide nanopowders prepared by chemical means. *Bull. Russ. Acad. Sci. Phys.* **79**, 1106–1112 (2015)
- Mercante, L.A., Melo, W.W.M., Granada, M., Troiani, H.E., Macedo, W.A.A., Ardison, J.D., Vaz, M.G.F., Novak, M.A.: Magnetic properties of nanoscale crystalline maghemite obtained by a new synthetic route. *J. Magn. Magn. Mater.* **324**, 3029–3033 (2012)
- Ramos Guivar, J.A., Bustamante, A., Flores, J., Mejía Santillan, M., Osorio, A.M., Martínez, A.I., De Los Santos Valladares, L., Barnes, C.H.W.: Mössbauer study of intermediate superparamagnetic relaxation of maghemite (γ -Fe₂O₃) nanoparticles. *Hyperfine Interact.* **224**, 89–97 (2014)
- Edelman, I., Ivanova, O., Ivantsov, R., Velikanov, D., Zabluda, V., Zubavichus, Y., Veligzhanin, A., Zaikovskiy, V., Stepanov, S., Artemenko, A., Curly, J., Kliava, J.: Magnetic nanoparticles formed in glasses co-doped with iron and larger radius elements. *J. Appl. Phys.* **112**, 084331 (2012)
- Reshetnik, E.I., Pakusina, A.P., Utochkina, E.A.: Studying of the structure of food additive lavitol-arabinogalactan and possibilities of its use as prebiotic. *Far. East Agrar. Bull.*, 16 (2010)